Research Article

Wenhao Yu, Weijun Yang, Pengwu Xu, Chunfa Dai, Qingsheng Liu, and Piming Ma*

Simultaneously enhance the fire safety and mechanical properties of PLA by incorporating a cyclophosphazene-based flame retardant

https://doi.org/10.1515/epoly-2022-0041 received December 28, 2021; accepted March 25, 2022

Abstract: The application of poly(lactic acid) (PLA) has been limited in flame-retardant field, and flame-retardant modification usually deteriorates its mechanical properties. In this study, a reactive flame-retardant hexa(ethylene oxide)-cyclotriphosphazene (HCCP-EP) was synthesized and used to improve the fire retardancy of PLA. As a result, the limiting oxygen index of PLA increased from 19.5% to 27.3% with an addition of 3 wt% HCCP-EP, and the PLA/HCCP-EP blend reached to underwriters laboratories (UL)-94 V-0 rating. The cone calorimeter test results showed that the peak heat release rate and total heat release of PLA decreased by 12.6% and 18.5%, respectively. Interestingly, the tensile strength of PLA increased slightly after the incorporation of HCCP-EP. The improved mechanical properties are ascribed to the fine dispersion of HCCP-EP and the coupling reaction between the epoxy groups of the HCCP-EP and the terminal groups of PLA during the melt processing.

Keywords: poly(lactic acid), cyclophosphazene-containing flame retardant, fire safety, mechanical properties

1 Introduction

Poly(lactic acid) (PLA), as a promising biodegradable polymer, has attracted extensive attention. The applications

* Corresponding author: Piming Ma, The Key Laboratory of Synthetic and Biological Colloids, Ministry of Education, Jiangnan University, 1800 Lihu Road, Wuxi 214122, China,

e-mail: p.ma@jiangnan.edu.cn

Wenhao Yu, Weijun Yang, Pengwu Xu: The Key Laboratory of Synthetic and Biological Colloids, Ministry of Education, Jiangnan University, 1800 Lihu Road, Wuxi 214122, China

Chunfa Dai: CSIC Pacli (Najing) Technology Co., Ltd, No. 31, Changqing Street, Najing, China

Qingsheng Liu: Key Laboratory of Eco-textiles of Ministry of Education, College of Textiles and Clothing, Jiangnan University, Wuxi, Jiangsu 214122, China

of PLA products focus on medical, agricultural, fabric, engineering, packing, electronic appliances, automotive materials, and textiles, etc. (1). However, the inherent flammability of PLA limits its applications in some special fields. Therefore, the flame-retarding modification of PLA is significant and necessary (2).

The flame retardants of PLA can be divided into intrinsic flame retardant and additive flame retardant (1). The intrinsic flame retardants will significantly improve the flame retardancy of PLA by bringing in a small number of flame-retardant groups or units by grafting or copolymerizing reactions. On the other hand, because of the low cost and easiness of processing, the additive flame retardants became more attractive. Up to now, different kinds of additive flame retardants for PLA have been reported, such as inorganic nano-sized, layered double hydroxides, phosphorus-based, and intumescent flame retardants (3-8). Wang et al. prepared a MOF flame retardant Ni-metal organic framework (Ni-MOF) and combined it with ammonium polyphosphate (APP) to modify PLA. The limiting oxygen index (LOI) of PLA composite increased to 31% with the presence of 1.7% Ni-MOF and 3.3% APP (9). Compared to other flame retardants, phosphorus-based flame retardants have been paid much attention in some industrial communities due to their high efficiency, low toxicity, and environment friendliness. The mechanism of phosphorus-based flame retardant includes four aspects: (i) when exposed to high temperature, phosphorus-based compounds can form stable polymers to cover the surface of the matrix, isolating oxygen and other combustible gases; (ii) the decomposition of phosphorus-based compounds can produce phosphoric acid, absorbing a large amount of heat and promoting the dehydration and carbonization of the polymer matrix; (iii) the decomposition of phosphorus-based compounds also produces phosphoruscentered radicals, which can capture hydroxyl, hydrogen, and other active groups, preventing the chain reaction in combustion and extinguishing the flame; and (iv) the phosphorus compounds can promote the degradation of the polymer matrix, which can extinguish the flame by

accelerating the dropping of polyesters while burning. Due to the multifarious flame-retardant mechanism, phosphorus-based flame retardants could be efficient and universal. The phosphorus-containing flame retardants have been widely studied in recent years (6,10-18). Chen et al. combined a phosphorus-containing flame retardant with APP at the ratio of 1:1; the LOI of PLA composite can reach 40%, while the total loading of additive was 25 wt% (19). Tao et al. reported a phosphazene cyclomatrix network polymer (PCPP); the PLA/PCPP composite reached UL-94 V-0 rating without dripping at 20 wt% loading of PCPP (20). Although these flame retardants enhance the flame retardancy of PLA conspicuously, their high loadings would damage the mechanical performance of PLA inevitably, which was dissatisfying during use. So, it is necessary to avoid the loss of mechanical properties during the flameretarding modification. Designing a efficient flame retardant can be an efficient path. Liu et al. reported a multifunctional flame retardant, which could improve the flame retardancy and crystallization rate at the same time. The LOI of PLA matrix reached 28.5% when the loading of flame retardant was 2.5% (21). Zhao et al. designed a superefficient flame retardant N,N'-diallyl-P-phenylphosphonicdiamide (P-AA); the LOI of PLA/P-AA blends reached 28.4% and the blends can pass UL-94 V-0 rating at only 0.5 wt% P-AA loading (22,23). Because of the little amount of addition, the tensile properties did not decline. In addition, adding other additives to improve the strength of flame-retardant PLA is also an effective method. Sypaseuth et al. added kenaf fibers to reinforce flame-retarded PLA, and the E modulus of PLA was increased to 6,740 MPa, while the neat PLA was only 3,650 MPa (24).

Employing reactive flame retardant is another efficient method as they can react with the matrix during processing without sacrificing the mechanical properties (25,26). PLA contains both hydroxyl groups and hydroxyl groups, making them have good reaction activity with epoxy groups.

Inspired by the studies mentioned above, a reactive flame-retardant hexa(ethylene oxide)-cyclotriphosphazene

(HCCP-EP) was designed and synthesized. HCCP-EP contains a cyclophosphazene structure and six epoxy groups. The cyclophosphazene structure contains alternating phosphorus and nitrogen atoms, providing a synergistic effect of phosphorus and nitrogen, which leads to good flame retardancy. The epoxy groups can react with the hydroxyl groups of PLA during the melt processing, which makes HCCP-EP playing the role of a chain extender. As a result, HCCP-EP can simultaneously enhance the flame retardancy and mechanical properties of PLA. This study may provide a potential route to extend the application range of PLA to the fields where both fire safety and superior mechanical performance were required.

2 Experiments

2.1 Materials

HCCP (98%) was purchased from Aladdin Corporation. Glycidol (97%) was purchased from Macklin Corporation. Tetrahydrofuran (THF, CP), potassium carbonate (K₂CO₃, AR), dichloromethane (CHCl₂, AR) were purchased from Sinopharm Chemical Reagent Corporation. PLA (3001D) was supplied by Nature Works Corporation.

2.2 Synthesis of HCCP-EP

The reaction formula is shown in Scheme 1. Glycidol (13.4 g, 0.18 mol), K_2CO_3 (12.42 g, 0.09 mol), and THF (100 mL) were placed into a 250 mL three-neck flask in N_2 atmosphere. Then, HCCP (10.44 g, 0.09 mol) was dissolved in THF (50 mL). The solution was added to the three-neck flask dropwise. The temperature was set as 65°C and the reaction took 48 h (27). After completing the reaction, the solid insoluble matter was removed

Scheme 1: The synthetic route of HCCP-EP.

out by vacuum filtration. The solvent was removed by reduced pressure distillation. The final product HCCP-EP was extracted by CHCl2 for three times with a yield of 70 wt%.

2.3 Synthesis of PLA/HCCP-EP blend

The samples with different HCCP-EP loadings were prepared by the melt processing. The processing contained two steps: (i) premixing PLA (50 g) with HCCP-EP (0.5, 1.5, and 2.5 g) and (ii) melt blending the mixture by a rheometer at 170°C with 50 rpm for 6 min. The samples were recorded as PLA/HCCP-EP-1, PLA/HCCP-EP-3, and PLA/HCCP-EP-5. The obtained mixture was placed in different sample modules, after preheating for 5 min and tableting for 1 min at 190°C, the final polymer sheets were obtained. As the control samples, the neat PLA was also prepared by the same process, while PLA and 5 wt% HCCP-EP were also mixed by solution (CHCl₃) casting and recorded as PLA/HCCP-EP-5(s).

2.4 Characterization

2.4.1 Fourier transform infrared (FT-IR) spectrometer

The FT-IR spectrum was detected on a FT-IR spectroscopy (Nicolet 6700, Thermo Fisher Scientific, USA), the range of resolution was 400–4.000 cm⁻¹ and the scan times were 32.

2.4.2 Nuclear magnetic resonance (NMR)

The ¹H NMR and ³¹P NMR were used to analyze the structure of HCCP-EP. The data were measured by NMR spectrometer (AVANCE III HD 400 MHz), and the solution was CDCl₃.

2.4.3 LOI

The LOI of PLA and PLA/HCCP-EP blend was measured by oxygen index meter (HC-2), the sample dimension was $100 \text{ mm} \times 10 \text{ mm} \times 4 \text{ mm}$ according to ASTM D2863-97.

2.4.4 Vertical burning test (UL-94)

The vertical burning test was tested by UL-94 vertical flame chamber (LX-4392, China), and the sample dimension was $100 \text{ mm} \times 13 \text{ mm} \times 3 \text{ mm}$ according to ASTM D3801.

2.4.5 Cone calorimeter test (CCT)

The fire behavior was evaluated by cone calorimeter according to ISO5660-1 under an external heat flux of 50 kW·m⁻², the sample dimension was $100 \text{ mm} \times 100 \text{ mm} \times 4 \text{ mm}$.

2.4.6 Thermogravimetry (TGA)

The decomposition behavior and thermal stabilities of HCCP-EP and PLA/HCCP-EP blend were analyzed by a TGA instrument (1100SF, Mettler-Toledo, Switzerland): the weight of the sample was around 5 (± 0.1) mg, the range of temperature was from 30°C to 600°C, and the step temperature rate was 20°C·min⁻¹. The flow of nitrogen was set as 50 mL·min⁻¹. The TGA was also used to analyze the thermal decomposition kinetics of PLA/HCCP-EP blend by using different heating rates (10, 20, 30, and 40°C·min⁻¹).

2.4.7 Energy dispersive X-ray spectroscopy (EDS)

The dispersibility of HCCP-EP in the PLA matrix was evaluated by an energy dispersive spectroscopy instrument (S-4800, HITACHI, Japan). The element mapping analysis of phosphorus (P) and nitrogen (N) was carried out. Before scanning, the surface of the sample was sprayed with gold using a sputter coater.

2.4.8 Rheological behavior

The rheological experiment was conducted on a DHR-2 rheometer (TA Instruments, USA) in a plate-plate configuration (25 mm in diameter and 1 mm in gap). The sample was heated to 190°C and kept for 50 min under a constant strain (1%) and frequency (1 Hz).

2.4.9 Thermogravimetry-infrared spectrometer (TG-IR)

The gas products of PLA/HCCP-EP blends were determined by TG-IR (PE TGA4000-SP2, USA). Testing condition: heating rate of 10°C·min⁻¹, N₂ atmosphere (50 mL·min⁻¹), temperature range from 30°C to 800°C, and wave number range from 500 to $4,000 \, \text{cm}^{-1}$.

2.4.10 Mechanical performance test

The tensile strength of PLA/HCCP-EP blend was measured by a double-column bench testing machine

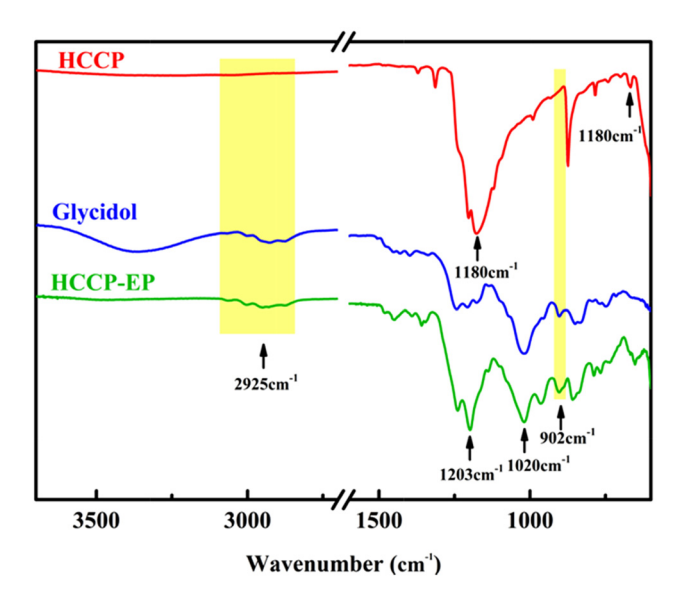


Figure 1: FT-IR spectra of HCCP, glycidol, and HCCP-EP.

(Instron 5967, USA); according to GB/T 1040-2006, the crosshead speed was set as 20 mm·min⁻¹, and the temperature was 23°C. Five specimens were tested for each sample. The notch impact strength of PLA/HCCP-EP blend was tested by a pendulum impact tester (HIT-2492, China); according to GB/T 1043.1-2008, the test temperature was 23°C, and five specimens were tested for each sample.

3 Results and discussion

3.1 Structural characterizations

The FT-IR spectra of HCCP, glycidol, and HCCP-EP are shown in Figure 1. The only characteristic peak of HCCP can be observed at $1,180 \, \text{cm}^{-1}$, which belongs to P=N

skeleton vibration. This peak also appears in the spectrum of HCCP-EP at 1,203 cm⁻¹ (28). This shift is owing to the change of chemical environment after the combination of glycidol with cyclotriphosphazene ring. In the spectrum of HCCP-EP, the peaks at 902 and 2,925 cm⁻¹ are assigned to the stretching vibration of -CH₂- and epoxy group, respectively (29). Especially, the peak at 1,020 cm⁻¹ belongs to the stretching vibration of P-O (15,30). What is more, the peak at 667 cm⁻¹ that belongs to P-Cl disappears in the spectrum of HCCP-EP, certifying the completion of the reaction. The ¹H NMR and ³¹P NMR of HCCP-EP are shown in Figure 2, which are consistent with the results in the literature (27). The results proved that the flame-retardant HCCP-EP has been synthesized successfully.

Before the melt processing, the thermostability of HCCP-EP was tested by TGA, and the result is shown in Figure A3 (Appendix). The $T_{5\%}$ and $T_{\rm dmax}$ of HCCP-EP were 208.3°C and 268.7°C, which meant HCCP-EP hardly decomposed during the melt processing.

After the PLA/HCCP-EP blend was prepared, FT-IR and rheological tests were carried out to prove the reaction between the epoxy groups of HCCP and the terminal groups of PLA while melt processing (Scheme 2). The FT-IR spectra of HCCP-EP, PLA, and PLA/HCCP-EP blends are shown in Figure 3a. The peak of epoxy groups can be observed obviously at 903 cm⁻¹ in the spectrum of HCCP-EP (29). After the melt processing, the peak of epoxy groups can hardly be found. To further prove the occurrence of the reaction, the following experiment was then implemented. PLA and 5 wt% HCCP-EP were dissolved into chloroform to produce PLA/HCCP-EP-5(s). The FT-IR spectra of PLA/HCCP-EP-5 and PLA/HCCP-5(s) are shown in Figure 3b.

Obviously, in the spectrum of PLA/HCCP-EP-5, the peak of the epoxy group was much weaker than that in the spectrum of PLA/HCCP-EP-5(s). The carbonyl group

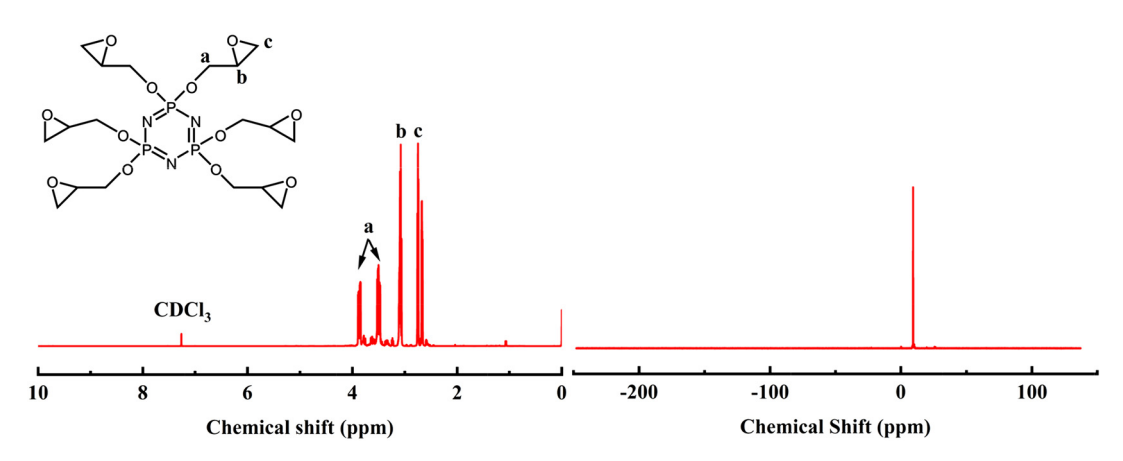


Figure 2: The ¹H NMR and ³¹P NMR spectra of HCCP-EP.

Scheme 2: Mechanism of the reaction between HCCP-EP and PLA.

was used as an internal standard to calculate the relative content, where the relative content of epoxy groups was 1.91% in PLA/HCCP-EP-5(s) and 0.42% in PLA/HCCP-5 (the calculation method is shown in Figure A2). The results showed that most of the epoxy groups had been consumed after the melt processing. What is more, the curves of complex viscosity at 190°C for PLA/HCCP-EP-5(s) are shown in Figure A4. Obviously, the complex viscosity of the sample increased with time and leveled off after about 2,700 s, which is corresponded to the reaction between the epoxy groups and PLA.

3.2 LOI and vertical burning tests

The flammability of PLA/HCCP-EP blends was measured by LOI and vertical burning tests (UL-94). The LOI results are shown in Figure 4. The LOI of PLA was 19.5% and increased to 25% when the loading of HCCP-EP was 1 wt% (PLA/HCCP-EP-1). Furthermore, the LOI reached 27.3%

when 3 wt% HCCP-EP was added (PLA/HCCP-EP-3). When 5 wt% HCCP-EP was loaded (PLA/HCCP-EP-5), the LOI reached 27.8%. The UL-94 test results are shown in Figure 5 and Table 1. For PLA, when the flame contacted the sample, it was ignited immediately and kept burning with serious dripping after removing the igniter. What is more, the degreasing cotton was also ignited immediately, which demonstrated the inflammability of PLA. When 1 wt% HCCP-EP was added, the sample can also be ignited and kept burning for 10.9 s; the burning dripping was less serious, and the molten drop did not ignite the degreasing cotton. When the loading of HCCP-EP increased to 3 wt%, the PLA/HCCP-EP blend can pass UL-94 V-0 rating; after being ignited, the sample extinguished within 3.6 s, the burning dripping became much lighter and did not ignite the cotton. Moreover, the sample cannot be ignited, and no molten drop was observed during the first ignition when the loading of HCCP-EP reached 5 wt%. This phenomenon may be owing to the catalytic dehydration of phosphoric acid, which was formed by the thermal decomposition of

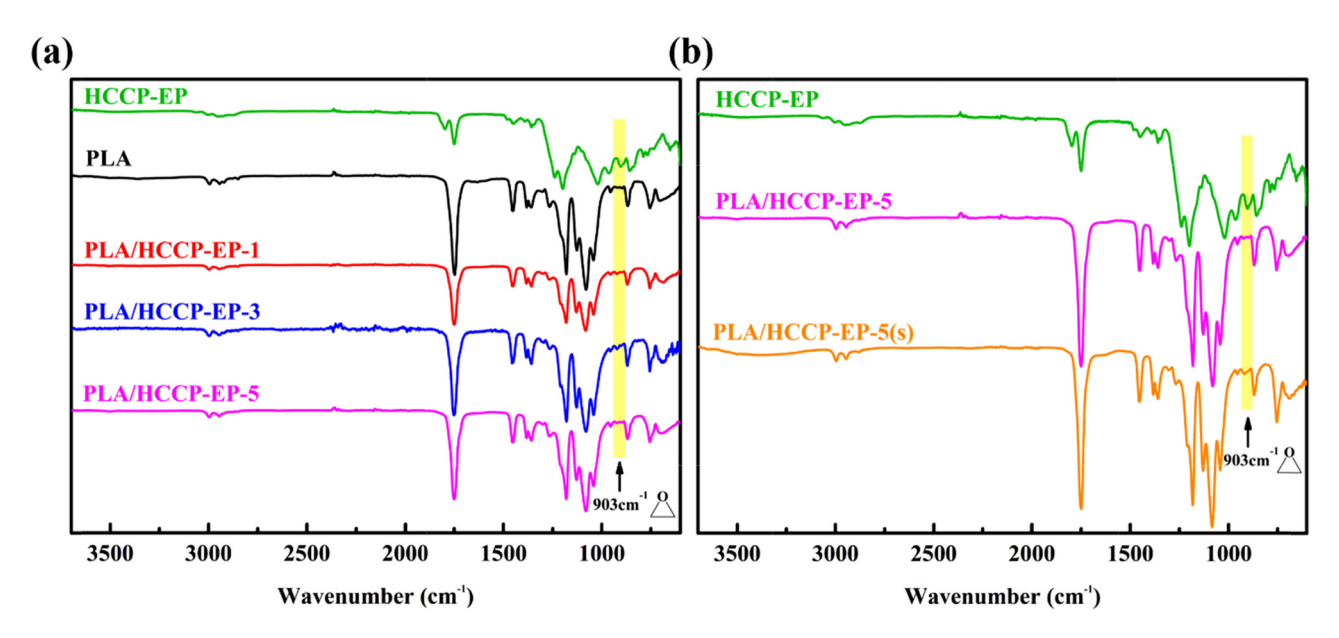


Figure 3: (a) The FT-IR of PLA/HCCP-EP blends. (b) The FT-IR of PLA/HCCP-EP-5 and PLA/HCCP-EP-5(s).

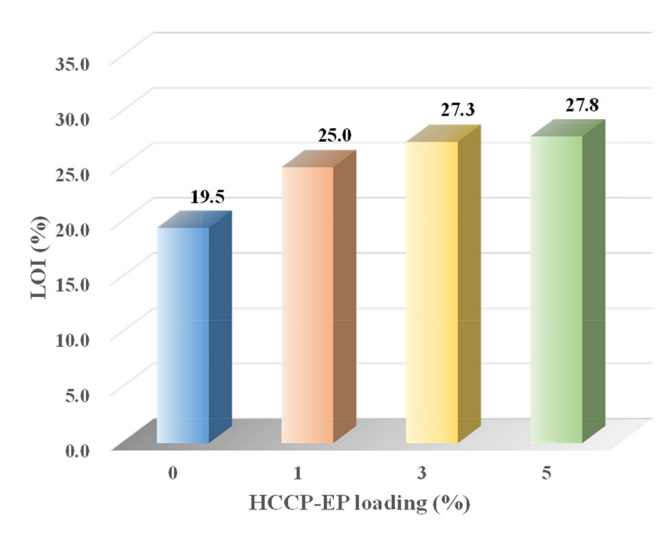


Figure 4: Results from LOI measurements for PLA/HCCP-EP blends.

HCCP-EP. Phosphoric acid catalyzed the PLA matrix to form a carbon layer, which can protect the unignited matrix and accelerate the extinguishment of the molten drop (31,32). As a whole, the addition of HCCP-EP can obviously improve the flame retardancy of PLA, which was mainly reflected in enhancing the value of LOI and self-extinguishing ability.

3.3 Fire behavior

The CCT is a frequently used method to measure the fire behavior of materials. Different from the LOI and UL-94 tests, which are used to simulate the fire scenario ignition, the CCT is employed to simulate developing fire. The



Figure 5: Results from UL-94 measurements for PLA/HCCP-EP blends: (a) PLA, (b) PLA/HCCP-EP-1, (c) PLA/HCCP-EP-3, and (d) PLA/HCCP-EP-5.

Table 1: The results of UL-94 tests for PLA/HCCP-EP blends

Sample	$t_1 + t_2$ (s)	Rating	Dripping	Ignition
PLA	>30	No rating	Serious	Yes
PLA/HCCP-EP-1	11.7	V-1	Serious	Yes
PLA/HCCP-EP-3	3.6	V-0	Light	Yes
PLA/HCCP-EP-5	0	V-0	Light	No

results from the CCT of PLA/HCCP-EP blends are shown in Figure 6 and Table 2. The curves of the heat release rate (HRR) of PLA and PLA/HCCP-EP-5 are shown in Figure 6a. For PLA, the HRR increased rapidly after being ignited and reached the peak value of 594.32 kW·m⁻² at 168 s, then began to decrease. While that of PLA/HCCP-EP-5 started to decrease 20 s earlier and the peak value was only 519.68 kW·m⁻². What is more, the total heat release (THR) reduced from 90.67 MJ·m⁻² for PLA to 76.89 MJ·m⁻² for PLA/HCCP-EP-5 (Figure 6b). These results may attribute

to the catalytic dehydration of phosphoric acid, which could catalyze matrix to form a carbon layer (11,31,33,34) and caused the residual mass (RM) raised from 7.6% to 24.4% as well (Figure 6c).

The results from CCTs are listed in Table 2. The time to ignition (TTI) of PLA/HCCP-EP-5 was 5 s earlier than PLA, which was owing to the addition of HCCP-EP caused the rise of system viscosity during the process of radiation heating, making the heat harder to diffuse (35). Effective heat of combustion (EHC) was the specific value of HRR and mass loss rate (MLR). EHC represents the amount of heat released by the combustible part of the decomposition volatiles during burning and can be used to determine the flame-retardant mechanism (36). The av-EHC of PLA/HCCP-EP-5 was 18.45 MJ·kg⁻¹, showing a slight decrease compared to PLA, which indicated that more nonflammable gas and less combustible gas were produced during the combustion of PLA/HCCP-EP-5. Last but not least, the av-MLR and peak CO₂ Y of PLA/HCCP-EP-5 were lower than PLA as well.

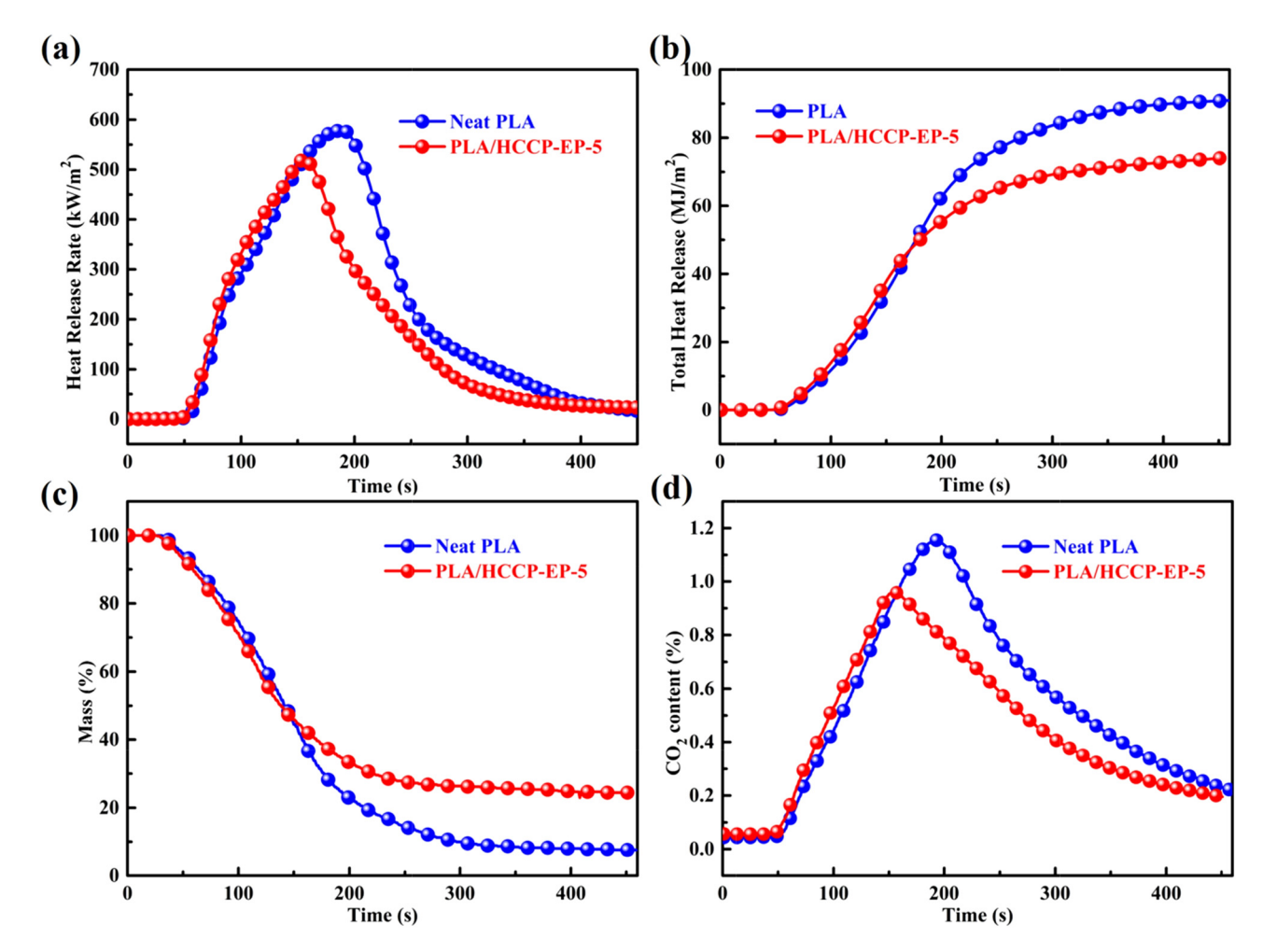


Figure 6: Fire safety performance of PLA and PLA/HCCP-EP-5 obtained from CCT. (a) HRR, (b) THR, (c) RM, and (d) CO₂ content (CO₂Y).

Table 2: The CCT results of PLA and PLA/HCCP-EP-5

Samples	TTI ^a (s)	PHRR ^b (kW·m ⁻²)	THR ^c (mJ·m ⁻²)	Average EHC ^d (MJ·kg ⁻¹)	Average MLR ^e (g·s ⁻¹ ·m ⁻²)	Peak CO ₂ Y ^f f (m ² ·m ⁻²)	RM ^g (%)
PLA	30	594.32	90.67	18.82	11.64	9.16	7.6
PLA/HCCP- EP-5	25	519.68	73.89	18.45	9.44	7.63	24.4

^aTime to ignition; ^bPeak heat release rate; ^cTotal heat release; ^dAverage effective heat of combustion; ^eAverage mass loss rate; ^fPeak CO₂ content; ^gResidual mass.

3.4 Gas phase analysis

To understand the flame-retardant mechanism of HCCP-EP, the evolved gaseous products of PLA and PLA/HCCP-EP-5 were collected and identified by TG-IR, the results are shown in Figure 7. The three-dimensional (3D) image of the evolved gaseous products of PLA and PLA/HCCP-EP-5 from TG-IR are shown in Figure 7a and b. The detailed FT-IR spectra of gaseous products of PLA and PLA/HCCP-EP-5 at different mass loss are shown in Figure 7c and d. As the results shown, the main gaseous products of PLA were H₂O (3,578 cm⁻¹), hydrocarbons (2,745 cm⁻¹), CO₂ (2,300 cm⁻¹), CO (2,183 and $2,113 \,\mathrm{cm}^{-1}$), and carbonyl compounds $(1,762 \,\mathrm{cm}^{-1})$. The characteristic peaks in fingerprint range belonged to C-H stretching (1,374 and 1,120 cm⁻¹) and C-O stretching $(1,243 \, \text{cm}^{-1})$ (22,37,38). The main gaseous products of PLA/HCCP-EP-5 were the same with those of PLA. Interestingly, in Figure 7d, the peak at 1,243 cm⁻¹ (C-O) is much weaker than that in Figure 7c, which can be observed more clearly in Figure 7e. According to reports in the literature, the decrease of this peak was related to the release of phosphorus-centered radicals such as PO (22). Moreover, a weak peak can be observed at 897 cm⁻¹ in Figure 7d and e, which belonged to P-O stretching (39,40). The appearance of P-O further proved the exist of phosphorus-centered radicals in the system, affording important evidences to the flame-retardant effects of HCCP-EP in gaseous phase. In addition, as Figure 7f shows, PLA/HCCP-EP-5 can produce more water vapor during pyrolysis than PLA, which is related to the catalytic dehydration of phosphoric acid.

According to the results from LOI, vertical burning test, CCT, and TG-IR, the fire safety of PLA was improved obviously after the incorporation of HCCP-EP. Based on the results, the probable flame-retardant mechanism of HCCP-EP can be concluded as (i) during burning, HCCP-EP produced phosphorus-centered radicals (HPO', PO', etc.) by thermal decomposition, which can annihilate H' and OH' radicals produced by the burning of PLA. The decrease of the amount of H' and OH' radicals would interrupt or slow

down the chain reaction of combustion. What is more, the thermal decomposition of PLA/HCCP-EP produced more H₂O, which can dilute the concentration of combustible gas and lead to lower temperature. (ii) The phosphoric acid, which was produced by the thermal decomposition of HCCP-EP, can catalyze PLA matrix to form a carbon layer. The phosphoric acid, metaphosphoric acid, and polyphosphazene can cover the surface of the matrix, protecting the PLA from further burning (12,29,33,41–43). All these mechanisms lead to higher LOI, better self-extinguishing ability, and lower peak heat release rate (PHRR) of PLA/HCCP-EP blends. The flame-retardant mechanism of HCCP-EP is shown in Figure 8. The dispersibility of HCCP-EP in PLA matrix was measured by a scanning electron microscope (SEM)-assisted EDS, and the results are shown in Figure 9. The EDS element analysis clearly showed the dispersibility of phosphorus and nitrogen in PLA/HCCP-EP blends. Both phosphorus and nitrogen dispersed in the PLA matrix homogeneously (44). As the loading of HCCP-EP increasing, the amount of phosphorus and nitrogen increased obviously (45), as expected.

3.5 Thermal decomposition behavior

The thermal decomposition process of PLA/HCCP-EP blends was investigated by TGA, and the results are shown in Figure 10. For PLA, $T_{5\%}$ was 322.5°C and $T_{\rm dmax}$ was 355.7°C. When HCCP-EP was added, both $T_{5\%}$ and $T_{\rm dmax}$ of PLA increased. The $T_{\rm dmax}$ for all samples increased about 10°C, which were 365.4°C, 366.0°C, and 366.5°C, respectively. $T_{5\%}$ for PLA/HCCP-EP-1 and PLA/HCCP-EP-3 increased about 7°C. But, interestingly, $T_{5\%}$ for PLA/HCCP-EP-5 was 323.2°C, increased only 0.7°C compared to PLA. This may originate from the decomposition of HCCP-EP. When the additive amount of HCCP-EP increased, the epoxy group would be excess, which may lead to the reduction of the reaction extent between part HCCP-EP molecule and PLA matrix (46). The decomposition temperature of this part of HCCP-EP would be lower than the part that reacted sufficiently,

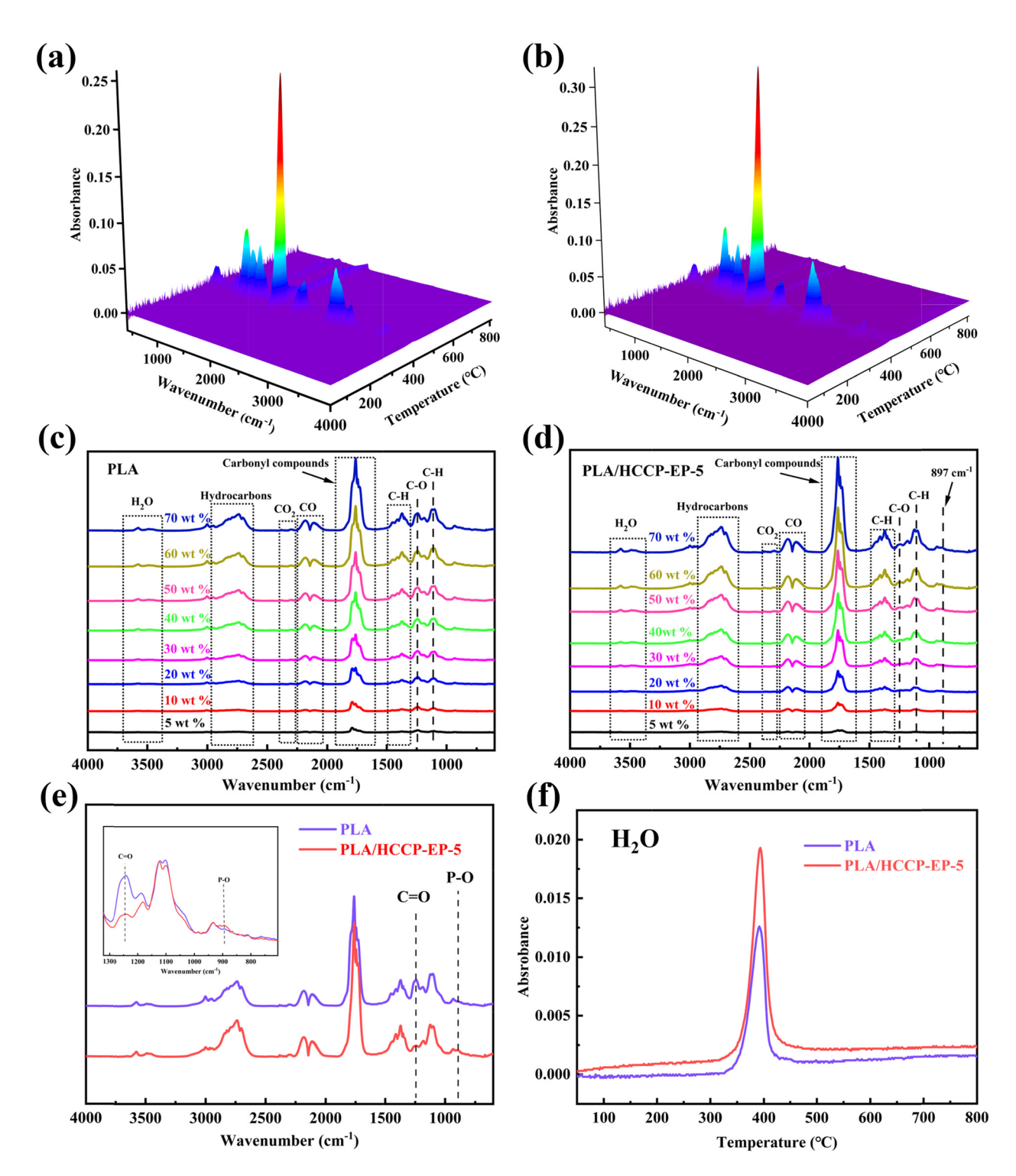


Figure 7: The 3D image of (a) TG-IR results for PLA and (b) PLA/HCCP-EP-5. FT-IR spectra of the gaseous products at different mass loss for (c) PLA and (d) PLA/HCCP-EP-5. (e) The FTIR spectra of gaseous products at a maximum decomposition rate. (f) Time-dependent FTIR spectra of H₂O at 3,578 cm⁻¹.

which caused the lower $T_{5\%}$. The increase of $T_{5\%}$ and $T_{\rm dmax}$ indicated that the PLA/HCCP-EP blends had better thermal stability than PLA, which was also related to the protective effects of the phosphoric acid, metaphosphoric acid, and polyphosphazene formed during high-temperature burning.

They covered the surface of the matrix and isolated heat, oxygen, and flame (47).

To further analyze the thermal decomposition behavior of PLA/HCCP-EP blends, a modified Kissinger method was adopted (22,48–51). The outline of the method was

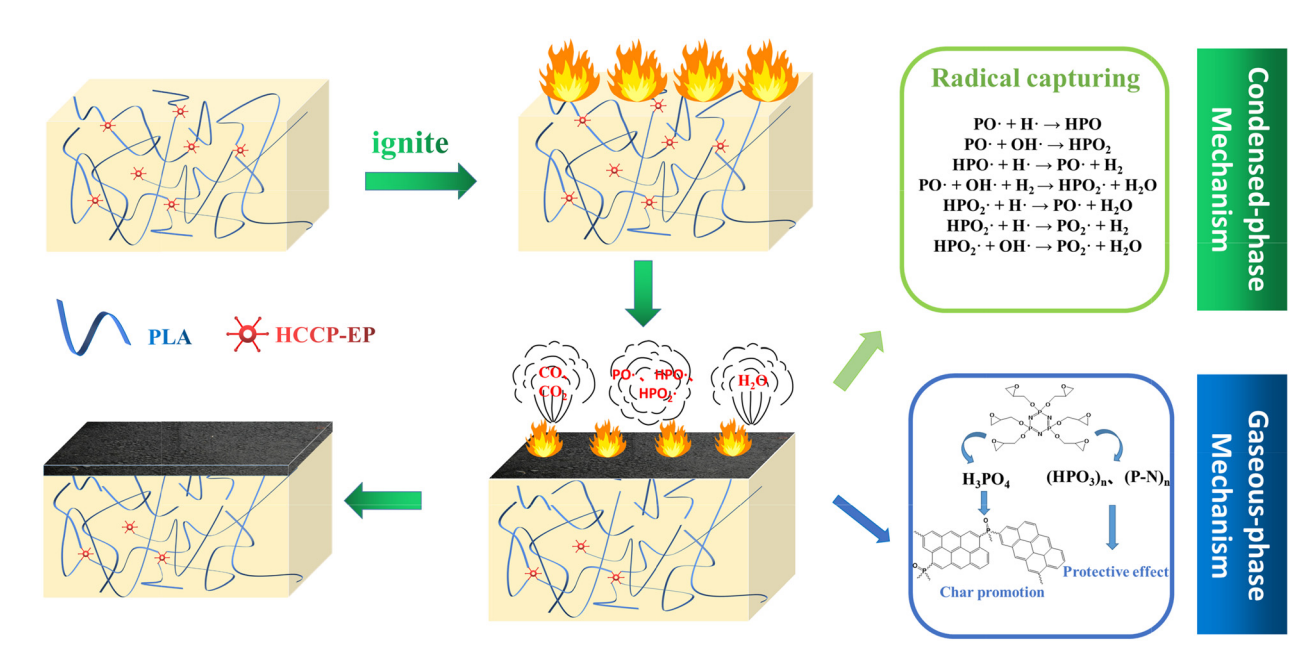


Figure 8: The flame-retardant mechanism of HCCP-EP.

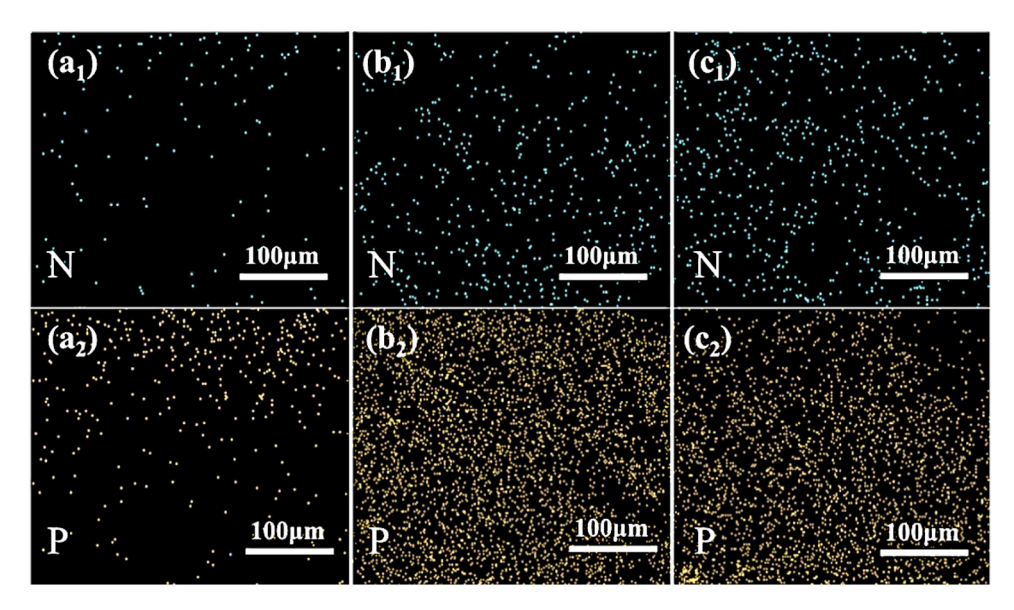


Figure 9: The SEM-assisted EDS mapping of P and N in $(a_1 \text{ and } a_2)$ PLA/HCCP-EP-1, $(b_1 \text{ and } b_2)$ PLA/HCCP-EP-3, and $(c_1 \text{ and } c_2)$ PLA/HCCP-EP-5.

given as follows. Based on a dynamic TGA process, most thermal decomposition reactions can be described by Eq. 1:

$$\frac{\mathrm{d}\alpha}{\mathrm{d}t} = Ae^{\left(-\frac{E}{RT}\right)}f(\alpha) \tag{1}$$

where α represents the fractional conversion in the solid reactant (α represents weight loss ratio here), A is

Arrhenius parameters, R is gas constant, T is the reactant temperature, $f(\alpha)$ is a so-called kinetic function that depends on the reaction mechanism, and E is the activation energy for the reaction. In nonisothermal experiments, the data were obtained under a different constant heating rate β (β = $\mathrm{d}T/\mathrm{d}t$), so that Eq. 1 can be written as follows:

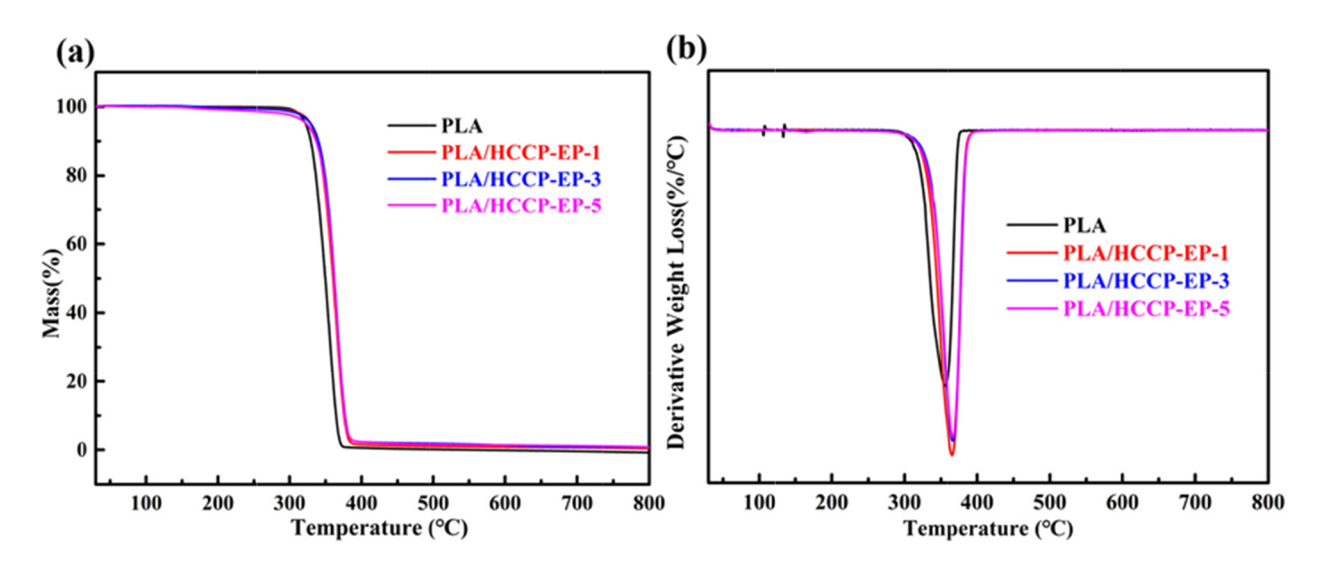


Figure 10: (a) TG and (b) DTG curves of PLA/HCCP-EP blends.

$$\frac{\mathrm{d}\alpha}{\mathrm{d}T} = \frac{A}{\beta} e^{\left(-\frac{E}{RT}\right)} f(\alpha) \tag{2}$$

After further calculation, the final equation for this isoconversional method can be described as Eq. 3:

$$\ln\left(\frac{\beta}{T^2}\right) = -\frac{E}{RT} + \ln\left(-\frac{AR(1 - 2RT/E)}{E\ln(1 - \alpha)}\right) \tag{3}$$

In Eq. 3, (1 - 2RT/E) can be assumed as a constant (22,44,45) so that the equation $\frac{d(\ln(\beta/T^2))}{d(1/T)} = -\frac{E}{R}$ was satisfied, which means that the value of activation energy corresponding to different fractional conversion α (recorded as E_{α}) can be obtained by plotting $\ln(\beta/T^2)$

against 1/T. The slope of the fitted curve was $-\frac{E_{\alpha}}{R}$, the value of E_{α} can be calculated by the slope obtained from each fitted curve under different fractional conversion α .

The fitted curve of $ln(\beta/T^2)$ against 1/T under different value of α for PLA and PLA/HCCP-EP-3 is shown in Figure 11, and the values of E_{α} are listed in Table 3. For both PLA and PLA/HCCP-EP-3, the value of E_{α} decreased as the increase of α , which means that the thermal decomposition became easier and easier as the reaction progressed. This may be because the molecular weight of PLA decreased after thermal decomposition. What is more, whether under high α or low α , E_{α} for PLA/HCCP-EP-3 was higher than that for PLA, which indicated that in the whole

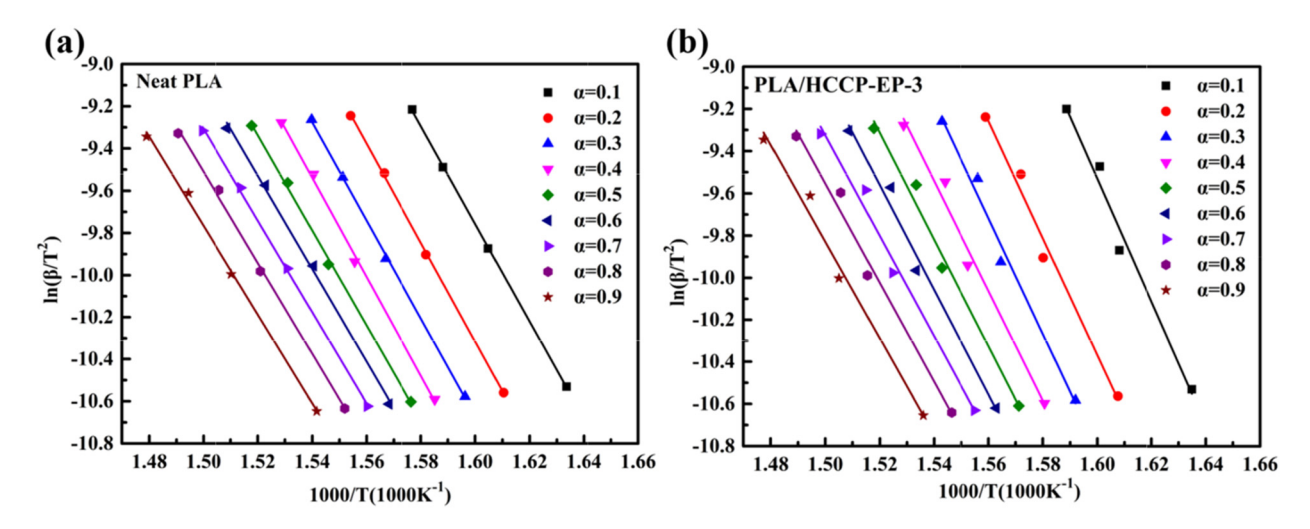


Figure 11: (a) Plot curves of $\ln(\beta/T^2)$ against 1/T of PLA under different α . (b) The plot curves of $\ln(\beta/T^2)$ against 1/T of PLA/HCCP-EP-3 under different α .

Table 3: Calculated E_{α} and r^2 of PLA and PLA/HCCP-EP-3 under different fractional conversion α

Α	PLA		PLA/HCCP-EP-3		
	E_{α} (kJ·mol ⁻¹)	r ²	E_{α} (kJ·mol ⁻¹)	r ²	
0.1	192.5	0.99979	243.1	0.97313	
0.2	195.3	0.99945	231.0	0.97828	
0.3	193.3	0.99939	228.7	0.98002	
0.4	195.6	0.99721	216.8	0.97444	
0.5	187.6	0.99797	210.4	0.97937	
0.6	183.7	0.99682	206.7	0.97885	
0.7	180.7	0.99873	197.9	0.97886	
0.8	179.6	0.99679	195.7	0.97830	
0.9	175.3	0.99675	190.8	0.98021	

thermal decomposition process, the thermal decomposition of PLA/HCCP-EP-5 was more difficult than PLA. Obviously, compared with PLA, PLA/HCCP-EP-3 showed a larger decrease in the value of E_{α} with the increase of α . For example, when α increased from 0.2 to 0.9, E_{α} of PLA

decreased to about 10.2%, from 195.3 to 175.3 kJ·mol $^{-1}$. While for PLA/HCCP-EP-3, E_{α} decreased to about 17.4%, from 231.0 to 190.8 kJ·mol $^{-1}$, which proved that the addition of HCCP-EP changed the decomposition route of PLA (22). Last but not least, at low α , for example, $\alpha = 0.3$, E_{α} was 228.7 kJ·mol $^{-1}$ for PLA/HCCP-EP-3, which was 35.4 kJ·mol $^{-1}$ higher than that of PLA. But when α increased to 0.9, the amount of increase decreased to 15.5 kJ·mol $^{-1}$. This can be explained by the decomposition of HCCP-EP. After being exposed to high temperatures for a long time, most of HCCP-EP was consumed, which made the restraint effect on the thermal decomposition weakened.

3.6 Mechanical properties

Figure 12 shows the results of relevant mechanical properties tests of PLA/HCCP-EP blends. Figure 12a-c shows

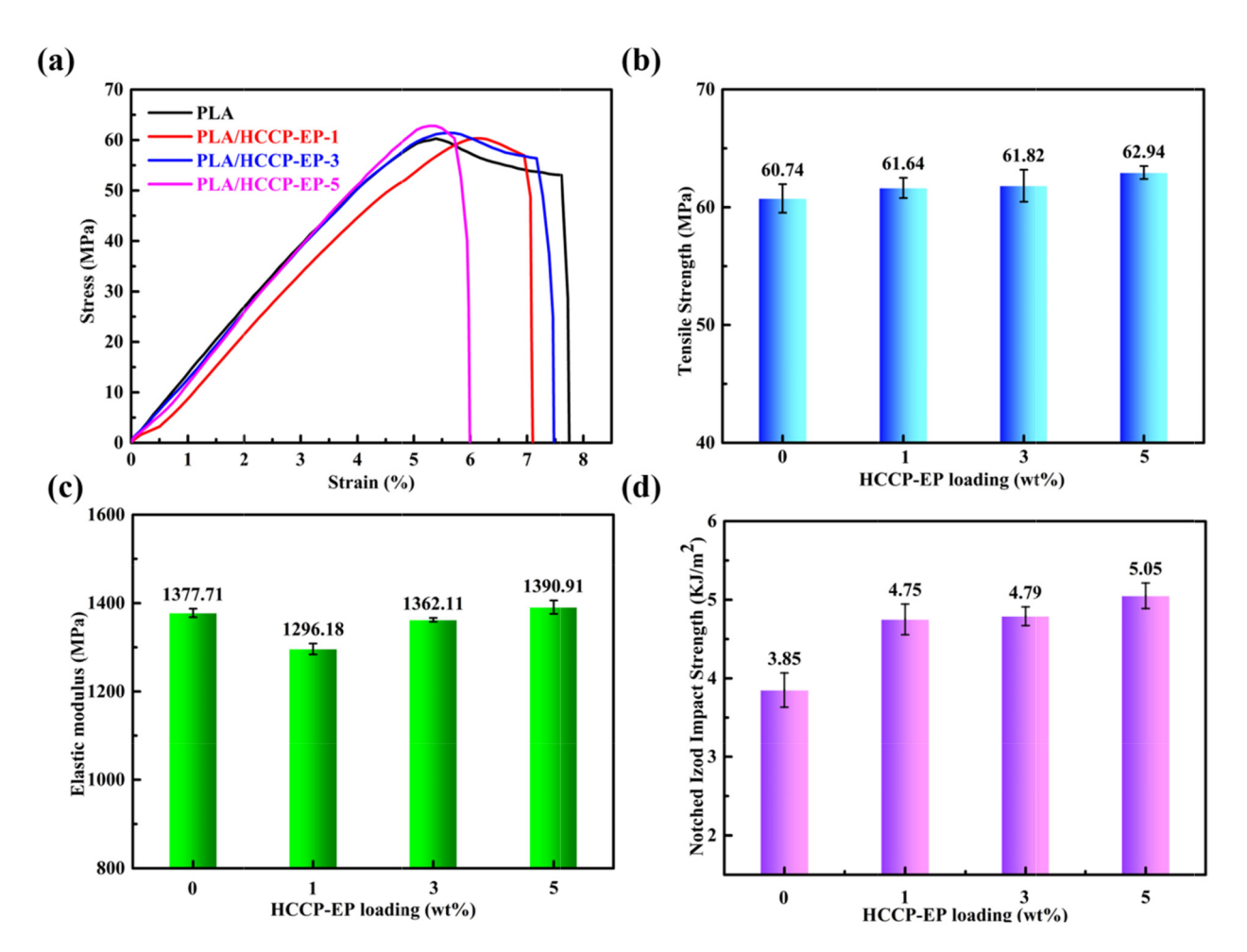


Figure 12: (a) Stress—strain curves of PLA and PLA/HCCP-EP blends. (b) Plots of tensile strength against loading of HCCP-EP. (c) Plots of elastic modulus against loading of HCCP-EP. (d) The notched izod impact strength of PLA/HCCP-EP blends.

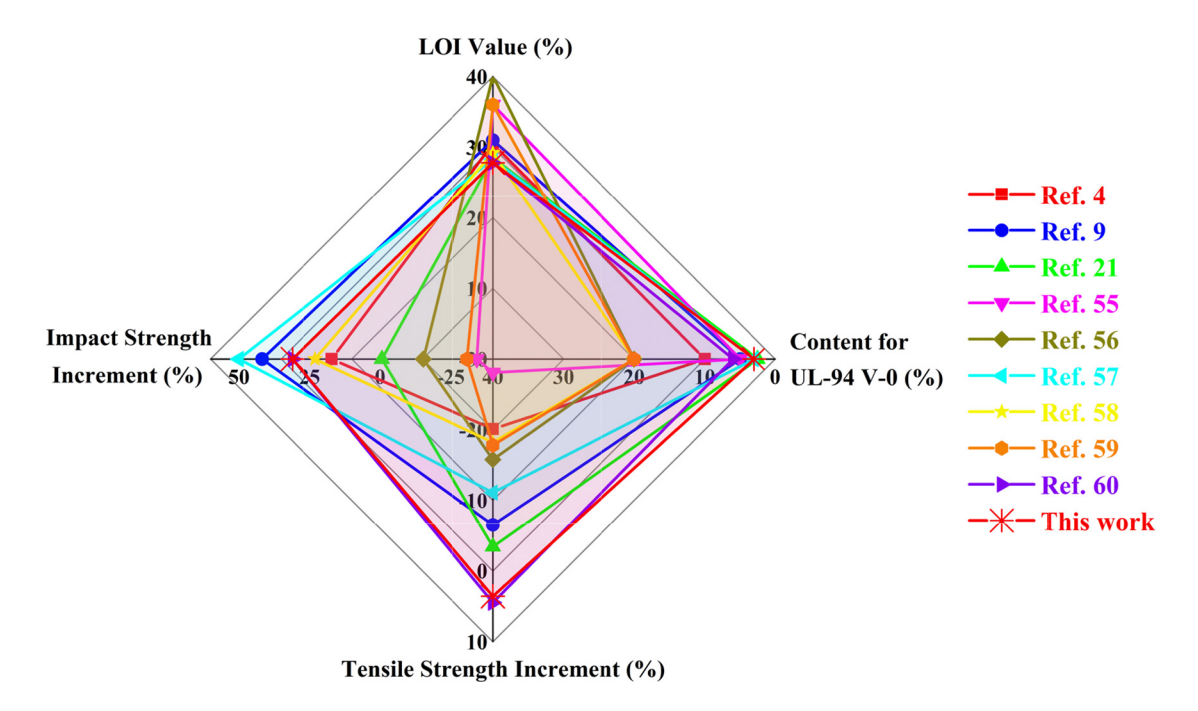


Figure 13: Comparison of the flame retardancy and mechanical properties between this study and relative literature in the recent years.

the stress-strain curves, tensile strength, and elastic modulus of PLA/HCCP-EP blends. As the loading of HCCP-EP increased, the tensile strength of PLA did not decline, even showed a slight rise. Meanwhile, the notched izod impact strength of PLA/HCCP-EP blends (Figure 12d) showed the same trend. Generally, the addition of flame retardant would sacrifice the mechanical properties of the matrix. In this case, when the epoxy group of HCCP-EP reacted with the terminal hydroxyl of PLA, HCCP-EP could work as a chain extender (Scheme 2), preventing the loss of mechanical properties (52-54).

The flame retardancy (LOI and UL-94) and mechanical properties of PLA/HCCP-EP blends are further compared with other reports in the literature (4,9,21,55–60), and the results are shown in Figure 13. It is obviously observed that, in this study, the additive content needed for UL-94 V-0 was lower than most of the systems, the increment of impact strength was higher than most of the systems. When it comes to tensile strength, compared with PLA, PLA/HCCP-EP blends showed a slight increase, while most of the other systems showed a decrease. However, the LOI value of this study was lower than many other systems, which needed further improvement.

4 Conclusion

In this study, a reactive cyclophosphazene-based flameretardant HCCP-EP was designed and synthesized. The results showed that the fire safety of PLA was enhanced obviously after the incorporation of HCCP-EP. Adding 3 wt% of HCCP-EP could increase the LOI of PLA increased from 19.5% to 27.3% and make PLA reached UL-94 V-0 rating. The phosphates produced by the thermal decomposition of HCCP-EP can catalyze PLA matrix to form a carbon layer, which will protect the PLA from further burning. Gas phase flame-retardant mechanism coexisted in this system due to the lower av-EHC of PLA/HCCP-EP-5 than that of PLA. Meanwhile, the addition of HCCP-EP slightly increased the activation energy (E_{α}) of PLA, which made the PLA more stabilized under high temperature. Furthermore, the addition of HCCP-EP would not compromise the mechanical properties of PLA. Especially, the notched izod impact strength of PLA/HCCP-EP-5 increased about 25% in comparison to PLA, which was mainly owing to the reaction between the epoxy groups of HCCP-EP and the terminal groups of PLA. We believe that this study may open a new trail for the preparation of high-performance PLA, which will broaden its applications in some fields such as textiles, furniture, and packaging.

Funding information: This work is supported by the National Natural Science Foundation of China (51873082, 52073123, 51903106), Distinguished Young Natural Science Foundation of Jiangsu Province (BK20200027).

Author contributions: Wenhao Yu: writing – original draft, formal analysis, data collection and analysis; Weijun Yang: investigation, formal analysis, writing – review and editing; Pengwu Xu: investigation, formal analysis; Chunfa Dai and Qingsheng Liu: data collection and analysis, writing – original draft preparation; Piming Ma: conceptualization, supervision, writing – review and editing.

Conflict of interest: The corresponding author of this article (Piming Ma) is a member of the Editorial Advisory Board of e-Polymers.

References

- (1) Kundu CK, Li Z, Song L, Hu Y. An overview of fire retardant treatments for synthetic textiles: from traditional approaches to recent applications. Eur Polym J. 2020;137:109911–72. doi: 10.1016/j.eurpolymj.2020.109911.
- Bourbigot S, Fontaine G. Flame retardancy of polylactide: an overview. Polym Chem-UK. 2010;1(9):1413–22. doi: 10.1039/ c0py00106f.
- (3) Zhang S, Yan Y, Wang W, Gu X, Li H, Li J, et al. Intercalation of phosphotungstic acid into layered double hydroxides by reconstruction method and its application in intumescent flame retardant poly (lactic acid) composites. Polym Degrad Stabil. 2018;147:142–50. doi: 10.1016/ j.polymdegradstab.2017.12.004.
- (4) Xiong Z, Zhang Y, Du X, Song P, Fang Z. Green and scalable fabrication of core-shell biobased flame retardants for reducing flammability of poly(lactic acid). ACS Sustain Chem Eng. 2019;7(9):8954-63. doi: 10.1021/acssuschemeng.9b01016.
- (5) Sypaseuth FD, Gallo E, Çiftci S, Schartel B. Polylactic acid biocomposites: approaches to a completely green flame retarded polymer. e-Polymers. 2017;17(6):449-62. doi: 10.1515/epoly-2017-0024.
- (6) Salmeia KA, Gooneie A, Simonetti P, Nazir R, Kaiser JP, Rippl A, et al. Comprehensive study on flame retardant polyesters from phosphorus additives. Polym Degrad Stabil. 2018;155:22–34. doi: 10.1016/j.polymdegradstab.2018.07.006.
- (7) Kang Bh, Lu X, Qu JP, Yuan T. Synergistic effect of hollow glass beads and intumescent flame retardant on improving the fire safety of biodegradable poly (lactic acid). Polym Degrad Stabil. 2019;164:167–76. doi: 10.1016/ j.polymdegradstab.2019.04.013.
- (8) Gao D, Wen X, Guan Y, Czerwonko W, Li Y, Gao Y, et al. Flame retardant effect and mechanism of nanosized NiO as synergist in PLA/APP/CSi-MCA composites. Compos Commun. 2020;17:170-6. doi: 10.1016/j.coco.2019.12.007.

- (9) Wang X, Wang S, Wang W, Li H, Liu X, Gu X, et al. The flamm-ability and mechanical properties of poly (lactic acid) composites containing Ni-MOF nanosheets with polyhydroxy groups. Compos Part B-Eng. 2020;183:107568–78. doi: 10.1016/j.compositesb.2019.107568.
- (10) Fang F, Ran S, Fang Z, Song P, Wang H. Improved flame resistance and thermo-mechanical properties of epoxy resin nanocomposites from functionalized graphene oxide via selfassembly in water. Compos Part B-Eng. 2019;165:406–16. doi: 10.1016/j.compositesb.2019.01.086.
- (11) Fiss BG, Hatherly L, Stein RS, Friščić T, Moores A. Mechanochemical phosphorylation of polymers and synthesis of flame-retardant cellulose nanocrystals. ACS Sustain Chem Eng. 2019;7(8):7951–9. doi: 10.1021/ acssuschemeng.9b00764.
- (12) Li S, Zhang Y, Li L, Zhang X. Synthesis of a phosphaphenanthrene/triazole oligomer for simultaneous improvement of flame retardancy and smoke suppression of epoxy resins. Compos Commun. 2021;28:100965–9. doi: 10.1016/ j.coco.2021.100965.
- (13) Li J, Yan X, Zeng X, Yi L, Xu H, Mao Z. Effect of trisilanolphenyl-POSS on rheological, mechanical, and flame-retardant properties of poly(ethylene terephthalate)/cyclotriphosphazene systems. J Appl Polym Sci. 2018;45912–23. doi: 10.1002/ app.45912.
- (14) Liu J, He Z, Wu G, Zhang X, Zhao C, Lei C. Synthesis of a novel nonflammable eugenol-based phosphazene epoxy resin with unique burned intumescent char. Chem Eng J. 2020;390:124620–30. doi: 10.1016/j.cej.2020.124620.
- (15) Mayer Gall T, Knittel D, Gutmann JS, Opwis K. Permanent flame retardant finishing of textiles by allyl-functionalized polyphosphazenes. ACS Appl Mater Inter. 2015;7(18):9349-63. doi: 10.1021/acsami.5b02141.
- (16) Pogorelčnik B, Pulko I, Wilhelm T, Žigon M. Influence of phosphorous-based flame retardants on the mechanical and thermal properties of recycled PC/ABS copolymer blends. J Appl Polym Sci. 2020;137(7):48377–89. doi: 10.1002/ app.48377.
- (17) Wang X, Yuan H, Lei S, Xing W, Lu H, Lv P, et al. Flame retardancy and thermal degradation mechanism of epoxy resin composites based on a DOPO substituted organophosphorus oligomer. Polymer. 2010;51(11):2435–45. doi: 10.1016/j.polymer.2010.03.053.
- (18) Liu C, Yang D, Sun M, Deng G, Jing B, Wang K, et al. Phosphorous-Nitrogen flame retardants engineering MXene towards highly fire safe thermoplastic polyurethane. Compos Commun. 2022;29:101055–61. doi: 10.1016/j.coco.2021.101055.
- (19) Chen Y, Wang W, Liu Z, Yao Y, Qian L. Synthesis of a novel flame retardant containing phosphazene and triazine groups and its enhanced charring effect in poly(lactic acid) resin. J Appl Polym Sci. 2017;134(13):44660–7. doi: 10.1002/app.44660.
- (20) Tao K, Li J, Xu L, Zhao X, Xue L, Fan X, et al. A novel phosphazene cyclomatrix network polymer: design, synthesis and application in flame retardant polylactide. Polym Degrad Stabil. 2011;96(7):1248–54. doi: 10.1016/j.polymdegradstab.2011.04.011.

- (21) Liu L, Xu Y, Pan Y, Xu M, Li B. Facile synthesis of an efficient phosphonamide flame retardant for simultaneous enhancement of fire safety and crystallization rate of poly (lactic acid). Chem Eng J. 2020;421:127761-75. doi: 10.1016/ j.cej.2020.127761.
- (22) Zhao X, Guerrero FR, Llorca J, Wang DY. New superefficiently flame-retardant bioplastic poly(lactic acid): flammability, thermal decomposition behavior, and tensile properties. ACS Sustain Chem Eng. 2016;4(1):202-9. doi: 10.1021/ acssuschemeng.5b00980.
- (23) Yang W, Zhao X, Fortunati E, Dominici F, Kenny JM, Puglia D, et al. Effect of cellulose nanocrystals on fire, thermal and mechanical behavior of N,N'-diallylphenylphosphoricdiamide modified poly(lactic acid). J Renew Mater. 2017;5(5):423-34. doi: 10.7569/JRM.2017.634146.
- (24) Sypaseuth F, Gallo E, Çiftci S, Schartel B. Polylactic acid biocomposites: approaches to a completely green flame retarded polymer. e-Polymers. 2017;17(6):449-62. doi: 10.1515/epoly-2017-0024.
- (25) Li A, Mao P, Liang B. The application of a phosphorus nitrogen flame retardant curing agent in epoxy resin. e-Polymers. 2019;19(1):545-54. doi: 10.1515/epoly-2019-0058.
- (26) Yu H, Xu X, Xia Y, Pan M, Zarshad N, Pang B, et al. Synthesis of a novel modified chitosan as an intumescent flame retardant for epoxy resin. e-Polymers. 2020;20(1):303-16. doi: 10.1515/ epoly-2020-0036.
- (27) Gouri ME, Bachiri AE, Hegazi SE, Rafik M, Harfi AE. Thermal degradation of a reactive flame retardant based on cyclotriphosphazene and its blend with DGEBA epoxy resin. Polym Degrad Stabil. 2009;94(11):2101-6. doi: 10.1016/ j.polymdegradstab.2009.08.009.
- (28) Jiang P, Gu X, Zhang S, Sun J, Wu S, Zhao Q. Syntheses and characterization of four phosphaphenanthrene and phosphazene-based flame retardants. Phosphorus Sulfur. 2014;189(12):1811-22. doi: 10.1080/ 10426507.2014.902828.
- (29) Liu R, Wang X. Synthesis, characterization, thermal properties and flame retardancy of a novel nonflammable phosphazenebased epoxy resin. Polym Degrad Stabil. 2009;94(4):617-24. doi: 10.1016/j.polymdegradstab.2009.01.008.
- (30) Li C, Ma C, Li J. Highly efficient flame retardant poly(lactic acid) using imidazole phosphate poly(ionic liquid). Polym Advan Technol. 2020;31(8):1765-75. doi: 10.1002/pat.4903.
- (31) Jia Y, Hu Y, Zheng D, Zhang G, Zhang F, Liang Y. Synthesis and evaluation of an efficient, durable, and environmentally friendly flame retardant for cotton. Cellulose. 2017;24(2):1159-70. doi: 10.1007/s10570-016-1163-z.
- (32) Yaoke D, Yuan Z, Wang J. Synthesis of a phosphorus-containing trisilanol POSS and its application in RTV composites. e-Polymers. 2018;18(3):237-45. doi: https://doi.org/10.1515/ epoly-2017-0204.
- (33) Zhang T, Cai Q, Wu D, Jin R. Phosphazene cyclomatrix network polymers: some aspects of the synthesis, characterization, and flame-retardant mechanisms of polymer. J Appl Polym Sci. 2010;95(4):880-9. doi: 10.1002/app.21295.
- (34) Krishnadevi K, Selvaraj V. Development of halogen-free flame retardant phosphazene and rice husk ash incorporated benzoxazine blended epoxy composites for microelectronic applications. New J Chem. 2015;39(8):6555-67. doi: 10.1039/ c5nj00364d.

- (35) Jiang P, Gu X, Zhang S, Sun J, Xu R, Bourbigot S, et al. Flammability and thermal degradation of poly (lactic acid)/ polycarbonate alloys containing a phosphazene derivative and trisilanollsobutyl POSS. Polymer. 2015;79:221-31. doi: 10.1016/j.polymer.2015.10.029.
- (36) Wang J, Qian L, Xu B, Xi W, Liu X. Synthesis and characterization of aluminum poly-hexamethylenephosphinate and its flame-retardant application in epoxy resin. Polym Degrad Stabil. 2015;122:8-17. doi: 10.1016/ j.polymdegradstab.2015.10.011.
- (37) Zou H, Yi C, Wang L, Liu H, Xu W. Thermal degradation of poly (lactic acid) measured by thermogravimetry coupled to Fourier transform infrared spectroscopy. J Therm Anal Calorim. 2009:97:929-35. doi: 10.1007/s10973-009-0121-5.
- (38) Fang Y, Miao J, Yang X, Zhu Y, Wang G. Fabrication of polyphosphazene covalent triazine polymer with excellent flame retardancy and smoke suppression for epoxy resin. Chem Eng J. 2020;385:123830-42. doi: 10.1016/j.cej.2019.123830.
- (39) Yu H, Xu X, Xia Y, Pan M, Zarshad N, Pang B, et al. Synthesis of a novel modified chitosan as an intumescent flame retardant for epoxy resin. e-Polymers. 2020;20(1):303-16. doi: 10.1515/ epoly-2020-0036.
- (40)Chen Y, Wu X, Qian L. Flame-retardant behavior and protective layer effect of phosphazene-triazine bi-group flame retardant on polycarbonate. J Appl Polym Sci. 2020;137:e49523-33. doi: 10.1002/app.49523.
- Chen Y, Wang W, Liu Z, Yao Y, Qian L. Synthesis of a novel flame retardant containing phosphazene and triazine groups and its enhanced charring effect in poly (lactic acid) resin. J Appl Polym Sci. 2017;134(13):44660-7. doi: 10.1002/app.44660.
- (42) Mathew D, Nair CR, Ninan KN. Phosphazene-triazine cyclomatrix network polymers: some aspects of synthesis, thermaland flame-retardant characteristics. Polym Int. 2000;49:48-56. doi: 10.1002/(SICI)1097-0126(200001) 49:1<48:AID-PI309>3.0.CO;2-M.
- (43) Nishita R, Kuroda K, Ota S, Endo T, Suzuki S, Ninomiya K, et al. Flame-retardant thermoplastics derived from plant cell wall polymers by single ionic liquid substitution. New J Chem. 2019;43(5):2057-64. doi: 10.1039/c8nj04797a.
- (44) Liu Y, Wang B, Ma S, Xu X, Qiu J, Li Q, et al. Phosphate-based covalent adaptable networks with recyclability and flame retardancy from bioresources. Eur Polym J. 2021;144:110236-47. doi: 10.1016/j.eurpolymj.2020.110236.
- (45) Zhang S, Chen H, Zhang Y, Zhang YM, Kan W, Pan M. Flame retardancy of high-density polyethylene composites with P, Ndoped cellulose fibrils. Polymers-Basel. 2020;12(2):336-50. doi: 10.3390/polym12020336.
- (46) Zhang C, Pan M, Qu L, Sun G. Effect of phosphorus-containing flame retardants on flame retardancy and thermal stability of tetrafunctional epoxy resin. Polym Advan Technol. 2015;26(12):1531-6. doi: 10.1002/pat.3576.
- (47) Li Z, Fernández Expósito D, Jiménez González A, Wang D-Y. Natural halloysite nanotube based functionalized nanohybrid assembled via phosphorus-containing slow release method: a highly efficient way to impart flame retardancy to polylactide. Eur Polym J. 2017;93:458-70. doi: 10.1016/ j.eurpolymj.2017.06.021.
- (48) Brown ME, Maciejewski M, Vyazovkin S, Nomen R, Mitsuhashi T. Computational aspects of kinetic analysis: Part A: the ICTAC kinetics project-data, methods and results.

- Thermochim Acta. 2000;355(s1-2):125-43. doi: 10.1016/S0040-6031(00)00443-3.
- (49) Yao F, Wu Q, Lie Y, Guo W, Xu Y. Thermal decomposition kinetics of natural fibers: activation energy with dynamic thermogravimetric analysis. Polym Degrad Stabil. 2008;93(1):90–8. doi: 10.1016/j.polymdegradstab.2007.10.012.
- (50) Kissinger HE. Reaction kinetics in differential thermal analysis. Anal Chem. 1957;29(11):1702-6. doi: 10.1021/ac60131a045.
- (51) Li CR, Tong BT. A new method for analysing non-isothermal thermoanalytical data from solid-state reactions. Thermochim Acta. 1999;325(1):43-6. doi: 10.1016/S0040-6031(98) 00568-1.
- (52) Al-Itry R, Lamnawar K, Maazouz A. Improvement of thermal stability, rheological and mechanical properties of PLA, PBAT and their blends by reactive extrusion with functionalized epoxy. Polym Degrad Stabil. 2012;97(10):1898-914. doi: 10.1016/j.polymdegradstab.2012.06.028.
- (53) Lu X, Lv Q, Huang X, Song Z, Xu N, Pang S, et al. Isothermal melt crystallization and performance evaluation of polylactide/thermoplastic polyester blends with multi-functional epoxy. J Appl Polym Sci. 2018;135(23):46343–53. doi: 10.1002/app.46343.
- (54) Wang X, Peng S, Chen H, Yu X, Zhao X. Mechanical properties, rheological behaviors, and phase morphologies of hightoughness PLA/PBAT blends by in-situ reactive compatibilization. Compos Part B-Eng. 2019;173:107028–37. doi: 10.1016/j.compositesb.2019.107028.

- (55) Wang X, He W, Long L, Huang S, Qin S, Xu G. A phosphorusand nitrogen-containing DOPO derivative as flame retardant for polylactic acid (PLA). J Therm Anal Calorim. 2021;145:331–43. doi: 10.1007/s10973-020-09688-7.
- (56) Chen Y, Wu X, Li M, Qian L, Zhou H. Construction of crosslinking network structures by adding ZnO and ADR in intumescent flame retardant PLA composites. Polym Advan Technol. 2022;33(1):198–211. doi: 10.1002/pat.5505.
- (57) Jia Y, Zhao X, Fu T, Li D, Guo Y, Wang X, et al. Synergy effect between quaternary phosphonium ionic liquid and ammonium polyphosphate toward flame retardant PLA with improved toughness. Compos Part B-Eng. 2020;197:108192. doi: 10.1016/j.compositesb.2020.108192.
- (58) Gu L, Qiu J, Qiu C, Yao Y, Sakai E, Yang L. Mechanical properties and degrading behaviors of aluminum hypophosphite-poly(Lactic Acid) (PLA) nanocomposites. Polym-Plast Technol. 2019;58(2):126–38. doi: 10.1080/03602559.2018.1466169.
- (59) Chen Y, Xu L, Wu X, Xu B. The influence of nano ZnO coated by phosphazene/triazine bi-group molecular on the flame retardant property and mechanical property of intumescent flame retardant poly (lactic acid) composites. Thermochim Acta. 2019;679:178336–43. doi: 10.1016/j.tca.2019.178336.
- (60) Zhang Y, Jing J, Liu T, Xi L, Sai T, Ran S, et al. A molecularly engineered bioderived polyphosphate for enhanced flame retardant, UV-blocking and mechanical properties of poly (lactic acid). Chem Eng J. 2021;411:128493–505. doi: 10.1016/ j.cej.2021.128493.

Appendix

The relative content of epoxy groups was obtained by calculating the area ratio of the characteristic peaks for epoxy group and carbonyl group in FT-IR absorbance spectra, respectively. The FT-IR absorbance spectrum of PLA/HCCP-EP-5 and PLA/HCCP-EP-5(s) is shown in Figure A2, and the integration method is shown in Figure A3. The calculation results are shown in Table A1. For PLA/HCCP-EP-5, the relative content of epoxy group is 0.42 (RC = $A_{EP}/A_{C=0}$ = 0.42), and for PLA/HCCP-EP-5(s), the relative content of epoxy group is 1.91% (RC = $A_{EP}/A_{C=O}$ = 1.91%).

Table A1: The calculation results of $A_{C=0}$, A_{EP}

Sample	$A_{C=0}$	A _{EP}
PLA/HCCP-EP-5	17.194	18.267
PLA/HCCP-EP-5(s)	0.072	0.349

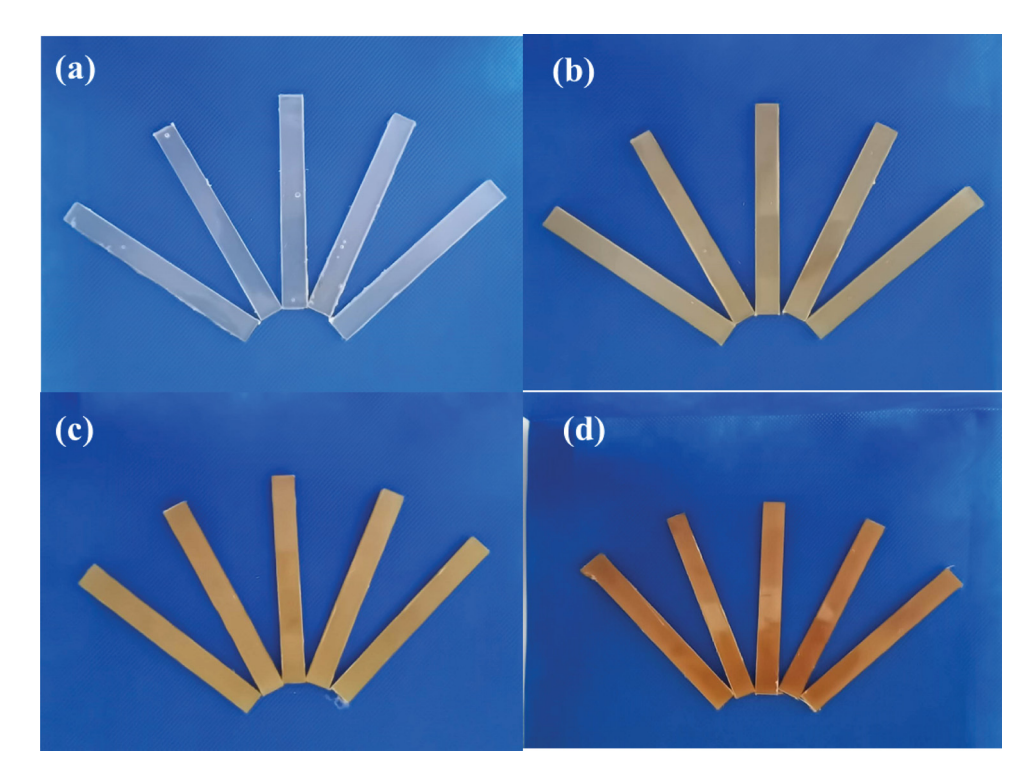


Figure A1: The sample of PLA/HCCP-EP composite for LOI test: (a) neat PLA, (b) PLA/HCCP-EP-1, (c) PLA/HCCP-EP-3, and (d) PLA/HCCP-EP-5. The sample was produced according to the standard GB/T2406-93.

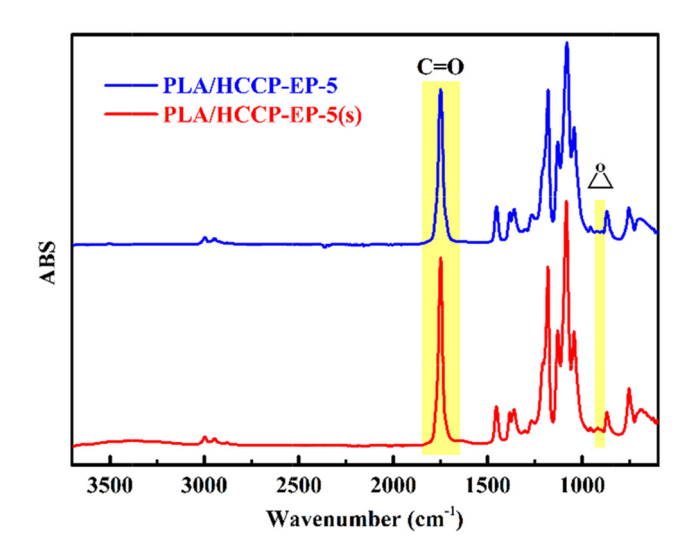


Figure A2: The FT-IR absorbance spectrum of PLA/HCCP-EP-5 and PLA/HCCP-EP-5(s).

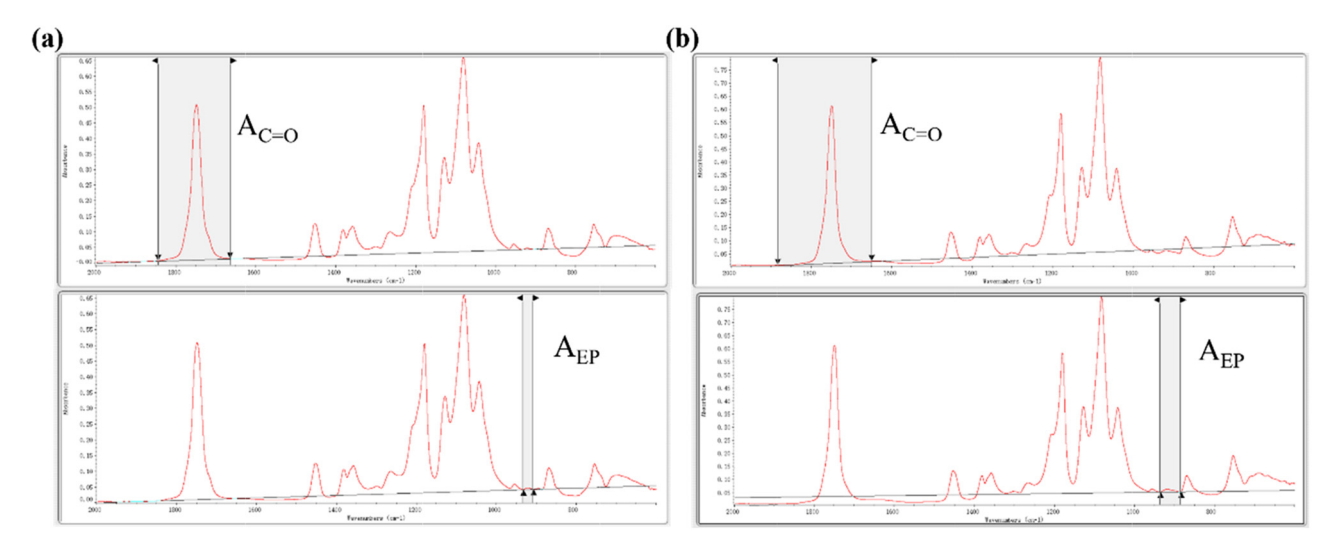


Figure A3: The corrected area of the characteristic peak for epoxy group and carbonyl group in the FT-IR absorbance spectra of (a) PLA/HCCP-EP-5 and (b) PLA/HCCP-EP-5(s).

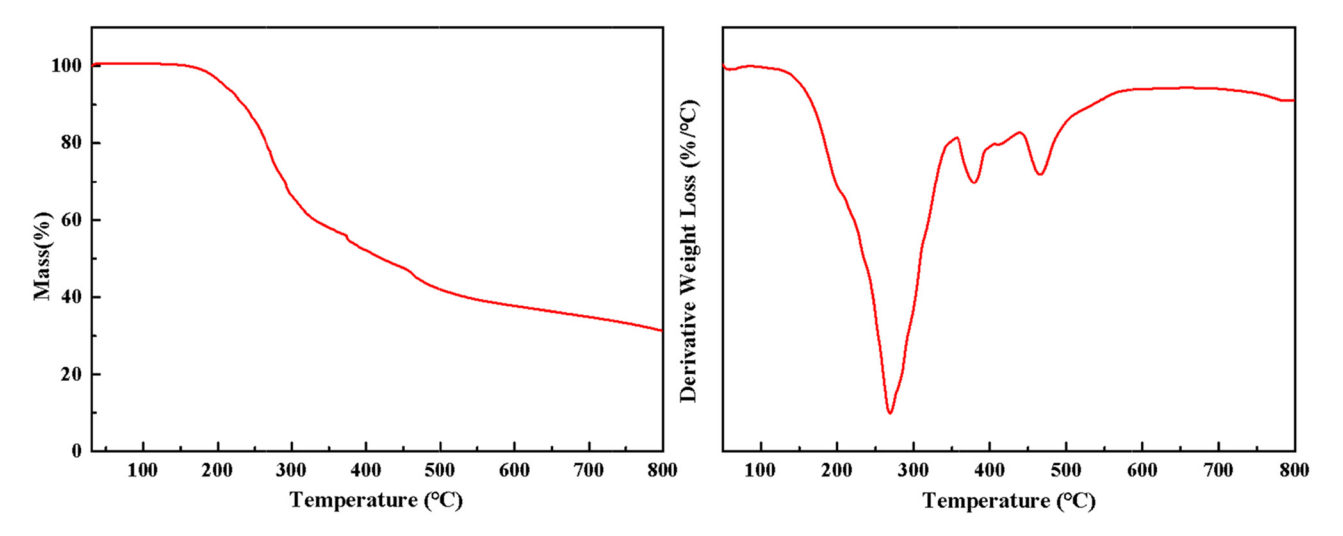


Figure A4: The TG and DTG curves of HCCP-EP.

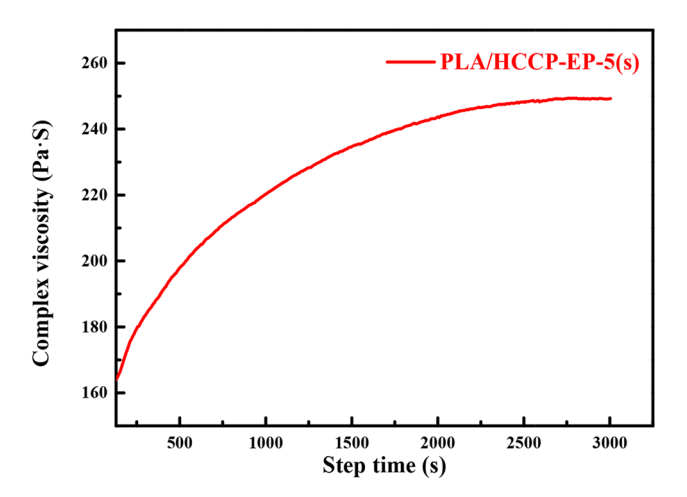


Figure A5: The curve of complex viscosity against step time at 170°C for PLA/HCCP-EP-5(s).